Chitin nanowhiskers with improved properties obtained using Natural Deep Eutectic Solvent and mild mechanical processing

Huy Vu Duc Nguyen, [a] Renko De Vries [a] and Simeon D Stoyanov*[a,b,c]

a.   *Laboratory of Physical Chemistry and Soft Matter, Agrotechnology & Food Sciences Group, Wageningen UR, Wageningen 6708WE, The Netherlands.*

b.   *Department of Chemical and Biomolecular Engineering, North Carolina State University, Raleigh, North Carolina 27695, United States*

c.   *Department of Mechanical Engineering, University College London, Torrington Place, London WC1E 7JE, U.K.*

Table of contents

1. Chemical composition characterization
2. Conductometric titration of ChNW suspensions and estimation of surface charge density
3. Appearance of PVOH-ChNW nanocomposites film
4. Mechanical properties of PVOH-ChNW nanocomposites

List of Figures:

Fig. S1. *^{13}C CP-MAS NMR spectra of native chitin powder, freeze-dried NADES-ChNW and Ac-ChNW powder.*

Fig. S2. Conductometric titration of NADES-ChNW (a); Ac-ChNW (b).

Fig. S3. Conductometric titration curve of NADES-ChNW suspension (0.1 wt%).

Fig. S4. (a) Digital picture of two sets of ChNW suspensions (A) Ac-ChNW and (B) NADES-ChNW.

Fig. S5. (a) Digital picture of PVOH nanocomposite films showing the transparency of PVOH nanocomposites film prepared with the same concentration of ChNWs (8wt%) prepared by acid hydrolysis and NADES, (b), (c) Bright-field images of the surface of PVOH nanocomposite film prepared with ChNW by acid hydrolysis and ChNWs prepared by NADES CM.

Fig. S6. Comparison of mechanical properties (a) Young's modulus; (b) Tensile strength and (c) Strain at break of the pure PVOH film, PVOH-(Ac-ChNW) and PVOH-(NADES-ChNW) composites film with various amounts of filler concentration.

List of Tables:

Table S1. Chemical shifts (ppm) of native chitin, freeze-dried NADES-ChNW and freeze-dried Ac-ChNW powder obtained by ^{13}C CP-MAS.

Table S2. Mechanical testing data of the pure PVOH film and PVOH-(NADES-ChNW) composites.

Table S3. Table S3. Onset temperature (t_{onset}) and degradation temperature (t_{max}), the residue mass of NADES-ChNW, pure PVOH film, and PVOH-ChNW nanocomposites.

1. Chemical composition characterization

The chemical fingerprints of native chitin powder and freeze-dried NADES-ChNW are characterized using ^{13}C CP-MAS NMR. The spectrum and chemical shifts are shown in Fig. S1 and Table S1, respectively.
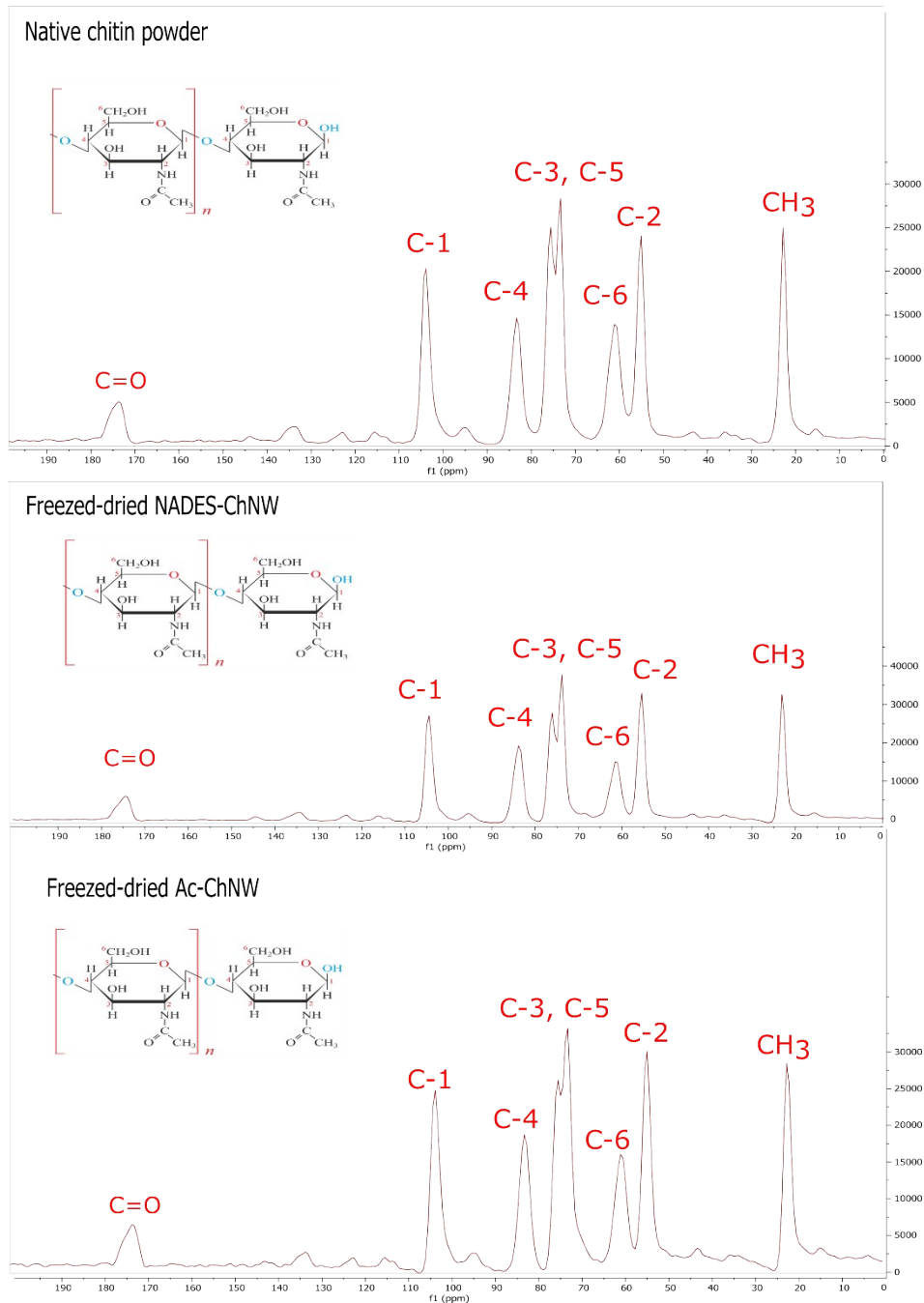
Fig. S1. ^{13}C CP-MAS NMR spectra of native chitin powder, freeze-dried NADES-ChNW and Ac-ChNW powder.

Table S1. Chemical shifts (ppm) of native chitin, freeze-dried NADES-ChNW and freeze-dried Ac-ChNW powder obtained by ^{13}C CP-MAS

	Sample		
	Native chitin	Freeze-dried NADES-ChNW	Freeze-dried Ac-ChNW
C=O	174.1	173.9	173.5
C1	103.9	103.9	103.7
C4	83.3	83.4	83.0
C3	75.9	75.9	75.1
C5	73.5	73.4	73.2
C6	61.0	61.0	60.6
C2	55.1	55.0	54.7
CH_3	22.8	22.8	22.3

2. Conductometric titration of ChNW suspensions and estimation of surface charge density

Both titration curves display three distinct regions. The first region, before the minimum in conductivity, corresponds to the neutralization of H+ still present from previously added HCl. The second region shows the minimum in the conductivity associated with the neutralization of the positive amino groups on the surface of the ChNW. After all amino groups are titrated, the pH value and conductivity increase proportionally to the amount of added OH-.
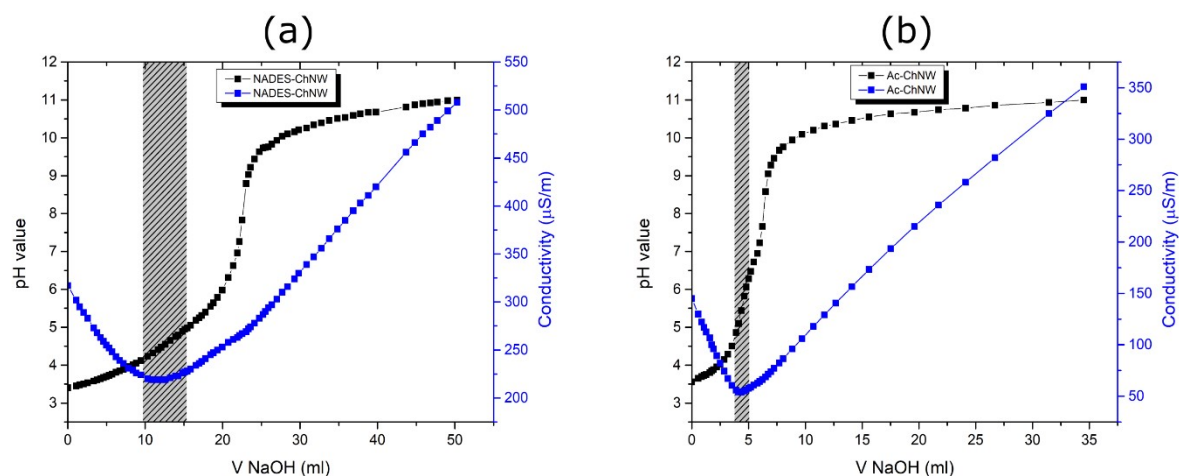
Fig. S2. Conductometric titration of NADES-ChNW (a); Ac-ChNW (b).

A key observation by comparing Figures 5 a and b for NADES-ChNW and Ac-ChNW is that the volume of base required to neutralize the positively charged amino group is much higher for NADES-ChNW

compared to Ac-ChNW. We quantified the density of the positively charged amino group on the surface of ChNW following established methods.

An example of calculating the surface charge density value of NADES-ChNW suspension is demonstrated in Fig. S3. The estimated surface charge density can be quantified using the established method.[1]
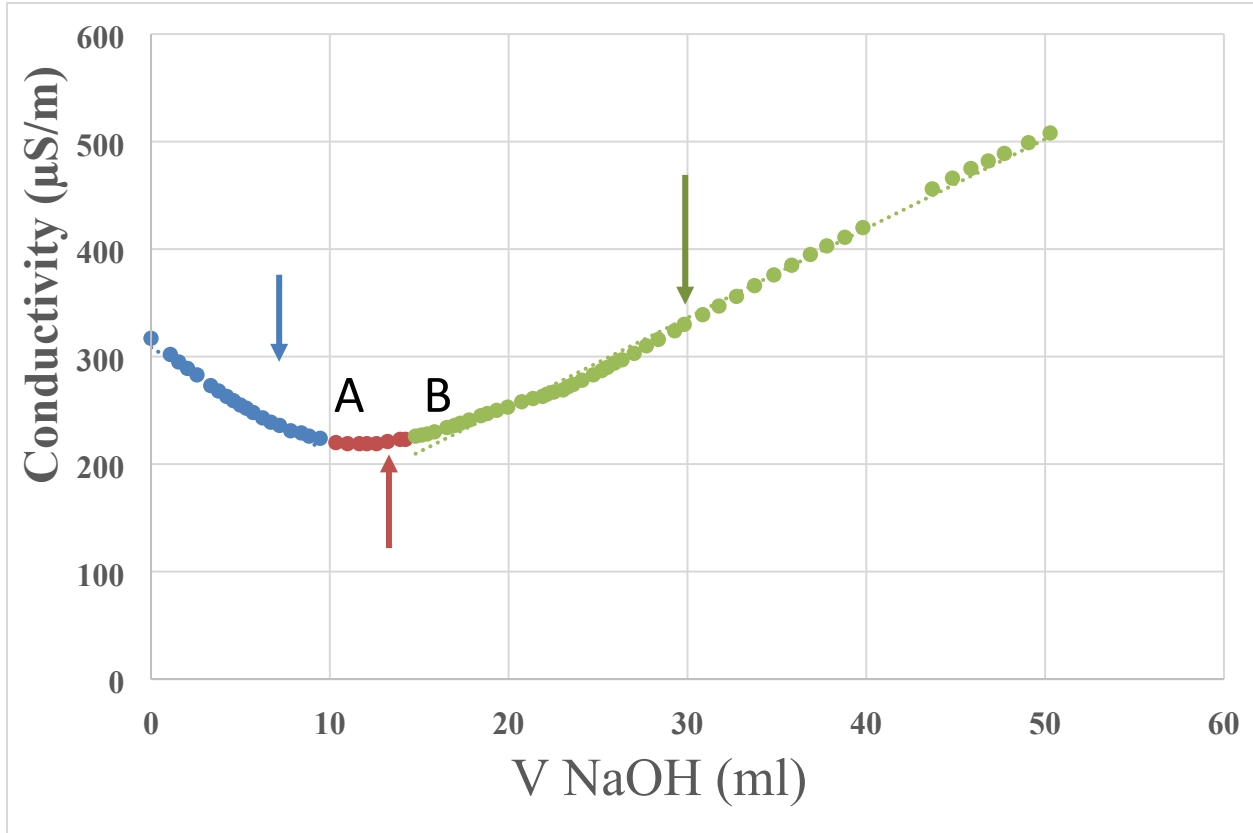
Fig. S3. Conductometric titration curve of NADES-ChNW suspension (0.1 wt%). The first region (in dark blue color) corresponds to the neutralization of H⁺ still present from previously added HCl. The second region (in brown color) shows the minimum in the conductivity associated with the neutralization of the positive amino groups on the surface of the NADES-ChNW. The third region (in green color) occurs after all amino groups are fully neutralized, associated with the neutralization of added amount of OH-.

We first determine the intersection points (A) and (B) between two straight lines, as shown in Fig. S3.

$$\text{(A)} \begin{cases} y = -0.9002x + 308.49 \\ y = 0.9942x + 208.07 \end{cases} \qquad \text{(B)} \begin{cases} y = 0.9942x + 208.07 \\ y = 8.3126x + 86.709 \end{cases}$$

Yielding the coordinates values:

A (9.22; 217.23) and B (16.58;224.56)

The volume of used NaOH to neutralize the positively charged amino groups on the surface of NADES-ChNW are calculated as the difference between these two values:

V NaOH = 16.58-9.22=7.36 (ml)

Knowing the volume of used titrant NaOH to fully neutralize the surface amino group and the amount of ChNW in the solution, we can estimate the surface charge density of these whiskers:

$$SCD = n_{NaOH} \frac{\rho \, V_{ChNW}}{mass_{ChNW}} \frac{1}{S_{ChNW}} \sim n_{NaOH} \frac{\rho \, D^2 L}{mass_{ChNW}} \frac{1}{DL} \sim n_{NaOH} \frac{\rho \, D}{mass_{ChNW}}$$

where: n_{NaOH} is the molar concentration of NaOH needed to neutralize the surface charge of chitin nanowhiskers with mass $mass_{ChNW}$, V_{ChNW} is the average volume of one chitin whisker, S_{ChNW} is its average surface area, ρ the density of the crystalline chitin, and D and L are the averaged nanowhisker diameter and length, respectively. The second term is inversely proportional to the total number of whiskers in solution, which multiplied by the surface of one whisker gives the total surface area of the whiskers. For high aspect ratio whiskers L/D>>1, we can approximate the volume of one whisker to be $V_{ChNW} \sim D^2 L$ and its surface area to be $S_{ChNW} \sim DL$.

(a) (b)
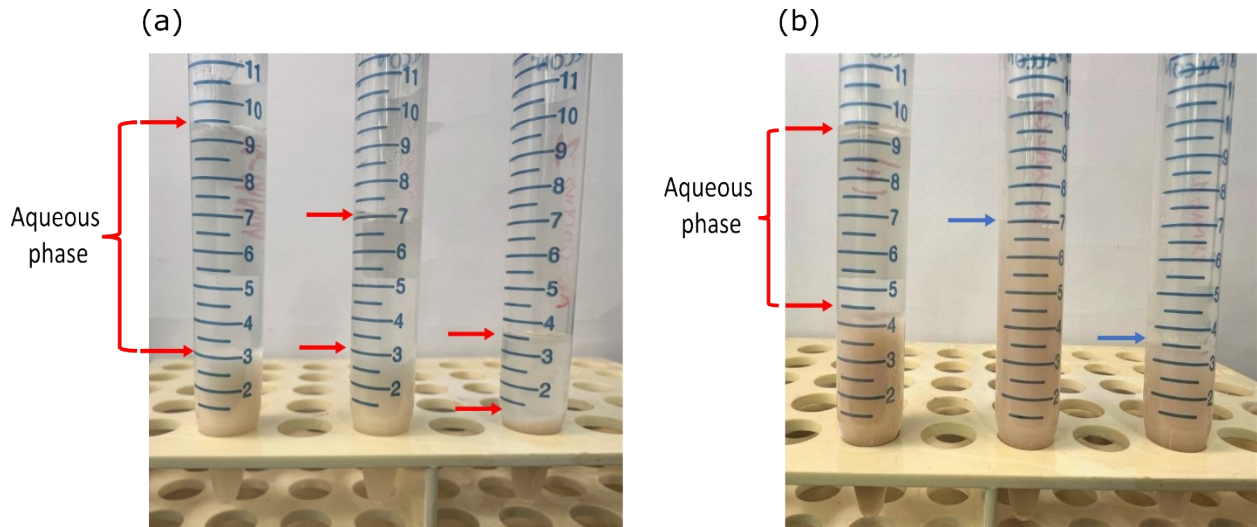
Fig. S4. Digital picture of two sets of ChNW suspensions (a) Ac-ChNW and (b) NADES-ChNW after 5 days. The initial concentration of ChNW suspensions is 5wt%, as shown in the far-right tube. The percolation threshold concentration is determined by dilution test when buffer pH 6 was added into the suspension until phase separation was observed in the tube. The blue arrow shows the final volume at which the suspension is still stable. The aqueous phase is marked within the red arrow, showing the phase separation of ChNW suspensions.

3. Appearance of PVOH-ChNW nanocomposites film
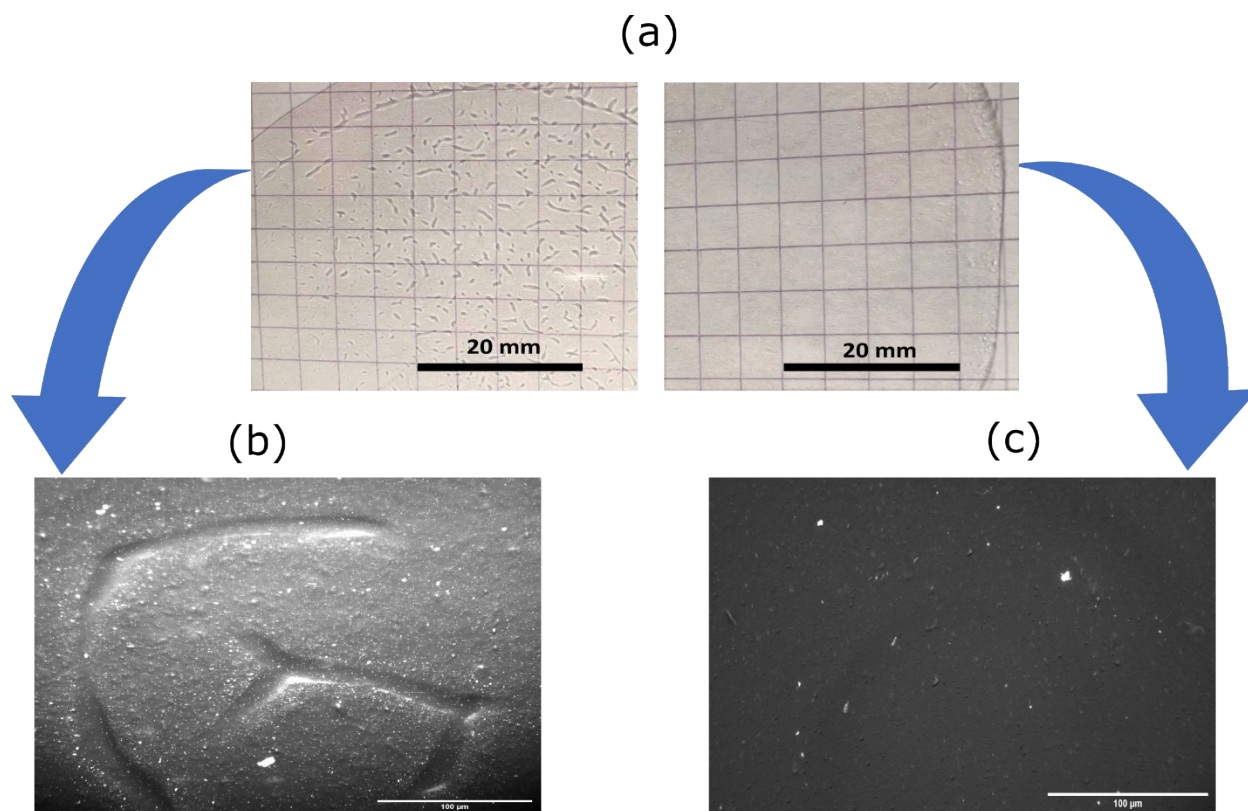
(a)

(b)   (c)

Fig. S5. (a) Digital picture of PVOH nanocomposite films showing the transparency of PVOH nanocomposites film prepared with the same concentration of ChNWs (8wt%) prepared by acid hydrolysis and NADES, (b), (c) Bright-field images of the surface of PVOH nanocomposite film prepared with ChNWs by acid hydrolysis and ChNWs prepared by NADES CM.

Both PVOH-ChNW composite films look similar in transparency (Fig. S3a), yet the composite film with NADES-ChNW filler appears much smoother than that with Ac-ChNW. As can be seen from Fig. S3(b, c), the PVOH-(NADES-ChNW) composite films showed a more uniform surface topography than the PVOH-(Ac-ChNW) composite film. The optical images denoted the topographical differences between these two PVOH nanocomposite films. Clear phase separation or presence of aggregates Ac-ChNW can be observed at relatively high ChNW loading content (8wt%, for instance). Fig. S3.b shows aggregates of Ac-ChNW, indicating the non-uniform distribution of chitin nanowhiskers in the PVOH matrix. These localized aggregations proved the non-homogenous distribution of Ac-ChNW within the PVOH matrix, especially at high loading concentrations. By contrast, there was no presence of aggregates on the surfaces of PVOH composites with the addition of NADES-ChNW. These observations indicate better uniformity of our prepared NADES-ChNW into the PVOH matrix. As explained in the main manuscript, it is linked to the better stability of NADES-ChNW suspension and its high compatibility and well-dispersion in the PVOH matrix.

4. **Mechanical properties of PVOH-ChNW nanocomposites**
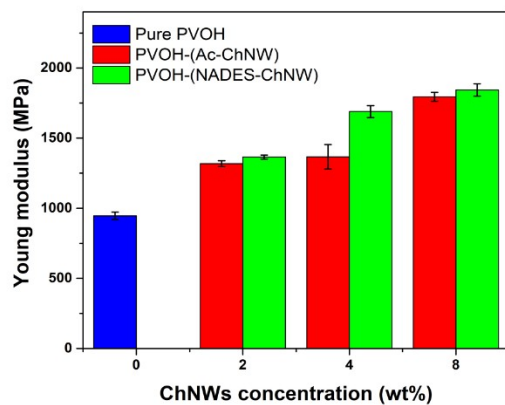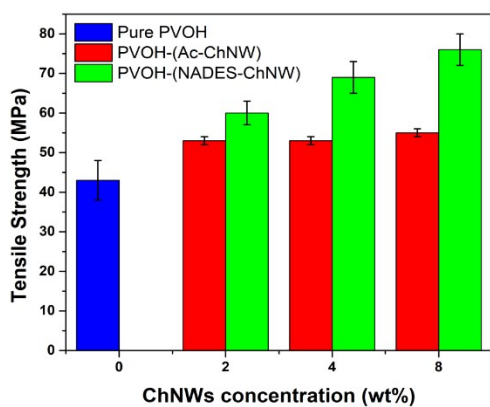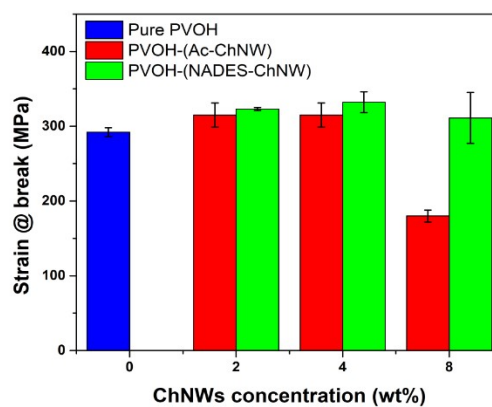
Fig. S6. Comparison of mechanical properties (a) Young's modulus; (b) Tensile strength and (c) Strain at break of the pure PVOH film, PVOH-(Ac-ChNW) and PVOH-(NADES-ChNW) composites film with various amounts of filler concentration.

Table S2. Mechanical testing data of the pure PVOH film and PVOH-ChNW composites.

Sample name	Modulus (MPa)	Tensile Strength	Strain at Break (%)
Pure PVOH	946 ± 25	43 ± 5	292 ± 6
PVOH-(NADES-ChNW)2wt%	1365 ± 14	60 ± 3	323 ± 2
PVOH-(NADES-ChNW)-4wt%	1689 ± 42	69 ± 4	332 ± 14
PVOH-(NADES-ChNW)-8wt%	1843 ± 43	76 ± 4	311 ± 34
PVOH-(Ac-ChNW)-2wt%	1284 ± 20	53 ± 1	315 ± 16
PVOH-(Ac-ChNW)-4wt%	1366 ± 87	53 ± 1	315 ± 16
PVOH-(Ac-ChNW)-8wt%	1795 ± 32	55 ± 1	180 ± 8

Table S3. Onset temperature (t_{onset}) and degradation temperature (t_{max}), the residue mass of NADES-ChNW, pure PVOH film, and PVOH-ChNW nanocomposites.

Sample name	t_{onset} (°C)	t_{max} (°C)	Mass of residue at 500 (°C) (%)
ChNws	250	390	17.7
Pure PVOH	280	345	8.8
PVOH-(NADES-ChNW)-10wt%	295	365	8.5
PVOH-(Ac-ChNW)-10wt%	285	355	6.3

Reference

1.   Farris, S.; Mora, L.; Capretti, G.; Piergiovanni, L., Charge density quantification of polyelectrolyte polysaccharides by conductometric titration: An analytical chemistry experiment. *Journal of Chemical Education* **2012,** *89* (1), 121-124.